

Anomalous phase diagram of the elastic interface with nonlocal hydrodynamic interactions in the presence of quenched disorder

Mohsen Ghasemi Nezhadhighi ^{*}

Department of Physics, School of Science, Shiraz University, Shiraz 71946-84795, Iran

 (Received 30 August 2023; revised 4 January 2024; accepted 29 January 2024; published 16 February 2024)

We investigate the influence of quenched disorder on the steady states of driven systems of the elastic interface with nonlocal hydrodynamic interactions. The generalized elastic model (GEM), which has been used to characterize numerous physical systems such as polymers, membranes, single-file systems, rough interfaces, and fluctuating surfaces, is a standard approach to studying the dynamics of elastic interfaces with nonlocal hydrodynamic interactions. The criticality and phase transition of the quenched generalized elastic model are investigated numerically and the results are presented in a phase diagram spanned by two tuning parameters. We demonstrate that in the one-dimensional disordered driven GEM, three qualitatively different behavior regimes are possible with a proper specification of the order parameter (mean velocity) for this system. In the vanishing order parameter regime, the steady-state order parameter approaches zero in the thermodynamic limit. A system with a nonzero mean velocity can be in either the continuous regime, which is characterized by a second-order phase transition, or the discontinuous regime, which is characterized by a first-order phase transition. The focus of this research is to investigate the critical scaling features near the pinning-depinning threshold. The behavior of the quenched generalized elastic model at the critical depinning force is explored. Near the depinning threshold, the critical exponent is obtained numerically.

DOI: [10.1103/PhysRevE.109.024115](https://doi.org/10.1103/PhysRevE.109.024115)

I. INTRODUCTION

The study of universal scaling behaviors associated with nonequilibrium critical phenomena is an attractive and fascinating field of statistical physics that has attracted considerable attention in recent years [1–5]. Indeed, it is expected that a wide range of models at the critical point could well be characterized by the same universal parameters, as is well known from equilibrium critical phenomena [6]. Is it possible to derive these parameters to determine the universality of critical phase transitions in out-of-equilibrium models? Recent studies have focused on the dynamical characteristics of a vast range of problems, including fracture propagation in solids [7–11], charge-density waves in anisotropic conductors [12,13], vortices in type-II superconductors [14], domain walls in ferromagnetic [15] or ferroelectric [16] systems, the contact line of a fluid drop on a disordered substrate [17–21], the deformation of crystals [11], crackling noise in a wide range of physical systems from magnetic materials to paper crumpling [22,23], friction and lubrication [24,25], the motion of geological faults [26], tumor growth [27,28], and many others. This diverse set of processes may be described as an extended elastic manifold driven over quenched disorder, which has a complicated dynamics that includes nonequilibrium phase transitions.

The competition between the deformation induced by quenched disorder (induced by the presence of impurities in the host environment) and the elastic material's response to

an applied driving force is the key factor determining their dynamical behavior in all of these complex nonlinear systems. The depinning transition phenomenon is a significant result of this competition [29]. In the absence of an external driving force F , the system is disordered but it does not move and remains pinned by the quenched disorder. When the external force is increased from zero, the elastic object unpins and reaches a finite steady-state velocity [2]. This describes the critical phase transition of the elastic interface at the critical force $F = F_c$, where the driving force F plays the role of the control parameter and the mean velocity v is the order parameter [1]. Note that the critical value of the external force F_c is not universal and its value depends on the details of the model. The steady-state average velocity follows a power-law characteristic as $v \sim (F - F_c)^\theta$ while approaching the critical point from above, where θ is a universal parameter. Other measures, such as the local width, the correlation functions, the correlation length, and the structure factor, may be used to extract the exponents associated with the criticality of the elastic interface. These techniques have been extensively used to investigate the self-affine surface structure's scaling properties [29–31].

Consider a single-valued function $u(\mathbf{x}, t)$ that describes an elastic interface. The global surface width $W = \sqrt{\langle [u(\mathbf{x}, t) - \langle u \rangle_{\mathbf{x}}]^2 \rangle_{\mathbf{x}}}$, is the simplest quantity used to characterize the scaling characteristics of elastic interfaces near the critical point, which is defined as the standard deviation around the mean position. For a finite system of size L , the roughening of u from a flat initial condition scales as

$$W(L, t) \sim t^\beta f(L/t^{1/\nu}), \quad (1)$$

^{*}mgnhaqiqi@gmail.com

where the exponents β and ν are called the growth and the dynamical exponent. The scaling function $f(x)$ is such that $f(x) \sim \text{const}$ for $x \gg 1$ and $f(x) \sim x^{\zeta_g}$ for $x \ll 1$ (the exponent ζ_g is known as the global roughness exponent). Finite-size effects, as expected, occur when $t_W^x \sim L^\nu$. The self-affine scaling relates now ζ_g , β , and the dynamical exponent ν through $\nu = \zeta_g/\beta$ [32].

The average velocity, which corresponds to the order parameter of the pinning-depinning transition of a driven interface, may be assumed to be a homogeneous function of time t and $|F - F_c|$, similar to critical phenomena, as

$$v(t, F) \sim t^{-\sigma} g(|F - F_c|t^{\sigma/\theta}), \quad (2)$$

where σ is a universal scaling exponent. For $F > F_c$ there is a crossover timescale $t_v^x \sim |F - F_c|^{\theta/\sigma}$ between two regimes: $g(x) \rightarrow \text{const}$ for $t \ll t_v^x$ and $g(x) \sim x^\theta$ for $t \gg t_v^x$. The equilibrium configuration of an elastic rough interface in the critical point is expected to be self-affine and the two-point correlation function is supposed to obey the scaling form

$$C(r) = \langle [u(\mathbf{x}) - u(\mathbf{x}')]^2 \rangle \sim |\mathbf{x} - \mathbf{x}'|^{2\zeta_l}, \quad (3)$$

where ζ_l is the local roughness exponent [32].

It is worth noting that the interface would satisfy a Family-Vicsek scaling only if $\alpha_l = \alpha_g$ were satisfied for some particular growth models. On the other hand, the growth models with $\alpha_l \neq \alpha_g$ could also be imaginable and represent dynamics with an anomalous scaling law. For instance, there are super-rough processes in which always $\alpha_l = 1$ but $\alpha_g > 1$. On the other hand, there are intrinsically anomalous roughened surfaces, for which $\alpha_l < 1$ and α_g can actually be any $\alpha_g > \alpha_l$ [32] (see also [33]). Various experimental, analytical, and numerical works have been proposed to compute the critical exponents θ , β , ζ_g , ζ_l , and σ characterizing the pinning-depinning phase transition, in a similar fashion to the equilibrium critical phenomena.

The purpose of this research is to describe and investigate the statics and dynamics of a generalized model for the investigation of a range of other reported phenomena in which the pinning-depinning phase transition may occur. The paper is organized as follows. Section II introduces the model. Section III describes the numerical formalism. In Sec. IV we discuss our findings. In Sec. V we summarize the results obtained and our conclusions.

II. DEFINITION OF THE MODEL

Despite the significant variations in theoretical models, many of the computations were performed using the linear assumption of the elasticity $u(\mathbf{x}, t)$. The following equation can be used to explain the motion of an interface in an isotropic disordered material at this level of precision [2]:

$$\frac{\partial u(\mathbf{x}, t)}{\partial t} = F + f_p(\mathbf{x}, u(\mathbf{x}, t)) - \mathcal{K}[u(\mathbf{x}, t)]. \quad (4)$$

Here F is a uniform external force which is also the control parameter and f_p represents the nonthermal quenched random forces due to the randomness and impurities of the heterogeneous medium. The quenched random noise $f_p(\mathbf{x}, u(\mathbf{x}, t))$ can be taken to have zero mean satisfying the relation $\langle f_p(\mathbf{x}, u) f_p(\mathbf{x}', u') \rangle = 2D\delta(\mathbf{x} - \mathbf{x}')\mathcal{R}(u - u')$, where

$\mathcal{R}(u - u')$ is assumed to decay rapidly for large values of its argument. The final term $\mathcal{K}[u(\mathbf{x}, t)]$ in Eq. (4) describes the elastic forces between different parts. It has the form

$$\mathcal{K}[u(\mathbf{x}, t)] = \int d^D \mathbf{x}' \int dt' \mathcal{J}(\mathbf{x} - \mathbf{x}', t - t') \times [u(\mathbf{x}', t') - u(\mathbf{x}, t)], \quad (5)$$

where D is the space dimension and $\mathcal{J}(\mathbf{x} - \mathbf{x}', t - t')$ is defined as the propagation kernel to transmit the stress on the interface from its elasticity. Moreover, systems with short-range elasticity of the interface are characterized by $\mathcal{J}(\mathbf{x}, t) \propto \delta(t)\nabla^2\delta(\mathbf{x})$ [2].

Theoretical studies on quenched disordered systems, such as a contact line of a liquid meniscus on a disordered substrate [18,34], crack propagation [34,35], and solid friction [36], have shown that it is possible to express the kernel $\mathcal{K}[u]$ in a long-range form

$$\mathcal{K}[u(\mathbf{x}, t)] \propto \int d^D \mathbf{x}' \frac{u(\mathbf{x}, t) - u(\mathbf{x}', t)}{|\mathbf{x} - \mathbf{x}'|^{D+z}}, \quad (6)$$

where the exponent z is a variable that depends on the model chosen to represent the elastic interface [10]. The most important aspect of the singular integration (6) is that it may be used to rewrite the elastic force $\mathcal{K}[u]$ as

$$\mathcal{K}[u(\mathbf{x}, t)] = (-\Delta)^{z/2} u(\mathbf{x}, t), \quad (7)$$

where $(-\Delta)^{z/2}$ is the fractional Laplacian defined by its Fourier transform $\widehat{(-\Delta)^{z/2}} \Phi(\mathbf{k}) = |\mathbf{k}|^z \widehat{\Phi}(\mathbf{k})$ [37]. According to Eqs. (4) and (7), one can rewrite Eq. (4) as

$$\frac{\partial u(\mathbf{x}, t)}{\partial t} = F + f_p(\mathbf{x}, u(\mathbf{x}, t)) - (-\Delta)^{z/2} u(\mathbf{x}, t). \quad (8)$$

It is indeed worth mentioning that the dynamics given by Eq. (8) is essentially a generalization of the quenched Edwards-Wilkinson (QEW) and quenched Mullins-Herring (QMH) equations, which are the simplest and most often used equations to explain the interface pinning-depinning transition in quenched random media, with $z = 2$ and 4 , respectively.

Analytical treatment of Eq. (8) is difficult due to the nonlinearity and heterogeneity of the pinning forces $f_p(\mathbf{x}, u(\mathbf{x}, t))$. The simplest hypothesis is to treat the problem perturbatively. The lowest-order approximation neglects important correlations in the growth direction implied by the dependence of the pinning force on the interface state. For this rough approximation, which was proposed by Blatter *et al.* [14], the pinning force can be simply replaced by an x -dependent but u -independent force. For $z = 2$ (quenched Edwards-Wilkinson model), by doing so one arrives at the so-called Larkin model

$$\frac{\partial u(\mathbf{x}, t)}{\partial t} = \nabla^2 u(\mathbf{x}, t) + F + f_p(\mathbf{x}). \quad (9)$$

Within the Larkin approximation the problem becomes linear and the critical exponents can be found exactly, by simple dimensional analysis, to obtain $\zeta_g = (4 - d)/2$ and $\nu = 2$, where d is the spatial dimension. By means of numerical simulations one finds $\zeta_g \approx 1.25$ and $\nu \approx 1.5$ in $d = 1$, which shows that the Larkin model is a good starting point to study the effects of disorder on kinetic roughening [38,39].

Much research has been carried out on the QEW and QMH equations, as well as the related models. Early studies investigated numerically the crucial characteristics of the QEW equation [40], which has been the subject of many theoretical and numerical studies in recent years [32,41–45]. Recently, a novel and very efficient approach investigated the QEW equation's depinning threshold and critical exponents [46,47].

The scaling properties of the QMH equation at the critical point of the pinning-depinning transition have been quantitatively explored [48–50]. It is worth noting that, for the so-called space-fractional quenched equation (8), the scaling hypothesis was established in Ref. [51] (the fractional power z is expected to be in the range $1.5 \leq z \leq 2$). The Grünwald-Letnikov form of a fractional derivative was used to discretize the space-fractional quenched equation, which is essentially an integro-differential equation, as noted in Ref. [51].

Despite the success of Eqs. (4) and (8) in describing the dynamics of elastic interfaces driven through a disordered medium, this toy model has one weakness: Hydrodynamic interactions are not included. This is the case, for instance, of polymers [52,53], membranes [54,55], the dynamics of colloid suspensions, macromolecular solutions, and multicomponent systems [56–60]. Because of the long-range hydrodynamic interaction, the dynamical behavior of these systems is correlated via flows.

The generalized elastic model (GEM), proposed in Ref. [61], is a suitable linear model that may capture the essence of criticality and phase transition (see [62–65] for more details). In this case, we use this model in the presence of a quenched disorder. The quenched form of the generalized elastic model (QGEM) is represented by the stochastic linear integro-differential equation

$$\frac{\partial u(\mathbf{x}, t)}{\partial t} = F + \int d^d x' \Lambda(|\mathbf{x} - \mathbf{x}'|) \frac{\partial^z}{\partial |\mathbf{x}'|^z} u(\mathbf{x}', t) + f_p(\mathbf{x}, u(\mathbf{x}, t)), \quad (10)$$

where the dynamical variables of the system $u(\mathbf{x}, t)$ describe an elastic interface driven through a disordered media, F is the driving force on the interface, and f_p represents the quenched pinning forces whose distribution can be chosen to be Gaussian with the first two moments $\langle f_p(\mathbf{x}, u) \rangle = 0$ and $\langle f_p(\mathbf{x}, u) f_p(\mathbf{x}', u') \rangle \propto \delta(\mathbf{x} - \mathbf{x}') \delta(u - u')$. The hydrodynamic interaction term $\Lambda(|\mathbf{x} - \mathbf{x}'|)$ corresponds to the nonlocal coupling of different sites \mathbf{x} and \mathbf{x}' . Here $\partial^z / \partial |\mathbf{x}|^z$ is the multidimensional Riesz-Feller fractional derivative operator, which is defined via its Fourier transform $\mathcal{F}\left\{\frac{\partial^z}{\partial |\mathbf{x}|^z} \Phi(\mathbf{x})\right\} \equiv -|\mathbf{k}|^z \Phi(\mathbf{k})$, immediately implying that the Riesz-Feller fractional derivative has the same meaning as the fractional Laplacian operator $\partial^z / \partial |\mathbf{x}|^z := -(-\Delta)^{z/2}$ [37].

At this point a specification of the hydrodynamic interaction kernel $\Lambda(\vec{r})$ is called for. For no fluid-mediated interactions, one may suppose that the friction kernel is local, $\Lambda(\vec{r}) = \delta(|\vec{r}|)$. This can be attributed to the interactions which are purely mechanical, for example, solid surfaces and fluctuating interfaces. For systems having nonlocal interactions, such as membranes, polymers, or viscoelastic surfaces, where the hydrodynamic interactions take on a long-range

power-law form, a different scenario

$$\Lambda(\vec{r}) \sim \frac{1}{|\vec{r}|^\alpha} \quad (11)$$

occurs (where $\frac{D-1}{2} < \alpha < D$) [61]. It should be emphasized that the D -dimensional Fourier transform of the hydrodynamic friction kernel (11) is given by $\Lambda(\mathbf{q}) = A|\mathbf{q}|^{\alpha-D}$ ($A = \text{const}$). It is clear that the local hydrodynamic interaction corresponds to the act of taking $\alpha = D$ and $A = 1$ [$\Lambda(\mathbf{q}) = 1$] [62]. We start by considering the Larkin approximation to find analytical expressions for the critical exponents ζ_g , ν , and β as functions of the control parameters α and z .

In this way we neglect the dependence on u in the pinning force $f_p(\mathbf{x}, u(\mathbf{x}, t)) = g(\mathbf{x})$. Then we construct a simple scaling theory based on dimensional analysis. The solution of the QGEM (10) has a continuous scale-invariant property, that is, the statistical properties of the interface field $u(\mathbf{x}, t)$ remain unchanged after rescaling of space and time according to the transformation

$$u(\lambda \mathbf{x}, \lambda^\nu t) = \lambda^{\zeta_g} u(\mathbf{x}, t), \quad (12)$$

where $\lambda > 1$ is an arbitrary scaling factor. This means that Eq. (10) does not change under scaling transformations $\mathbf{x} \rightarrow \lambda \mathbf{x}$ and $t \rightarrow \lambda^\nu t$, together with the corresponding rescaling in the amplitude $u \rightarrow \lambda^{\zeta_g} u$. By imposing the scaling transformation on the Larkin representation of Eq. (10) we get

$$\frac{\partial u(\mathbf{x}, t)}{\partial t} = \lambda^{d-\alpha-z+\nu} \int d^d x' \Lambda(|\mathbf{x} - \mathbf{x}'|) \frac{\partial^z}{\partial |\mathbf{x}'|^z} u(\mathbf{x}', t) + \lambda^{-d/2+\nu-\zeta_g} g(\mathbf{x}). \quad (13)$$

The scale invariance of the solution of Eq. (13) implies that $\nu = z + \alpha - d$ and $\zeta_g = \frac{2\nu-d}{2}$.

The next section presents a detailed description of the discretization approach used to numerically explore the generalized elastic model in the presence of quenched disorder (10) for various values of the fractional order z and the nonlocal hydrodynamic interaction strength α .

III. NUMERICAL ALGORITHM

We consider here the QGEM (10) in one spatial dimension $D = 1$. The interface position $u(x_i, t_n)$ is specified on a lattice of size L , where $x_i = i\Delta x$ and $t_n = n\Delta t$ are defined with $i = 0, \dots, L$ and u_i^n is kept as a continuous variable.

To solve Eq. (10) in discretized time and space, we use the finite-difference approximation to estimate the time derivative (forward Euler method)

$$\frac{\partial u(x_i, t_n)}{\partial t} = \frac{u(x_i, t_{n+1}) - u(x_i, t_n)}{\Delta t}. \quad (14)$$

The discrete-space Riesz-Feller fractional operator $\partial^z / \partial |x|^z$ in Eq. (10) can be approximated using the matrix transform method proposed by Ilic *et al.* [66,67]. Moreover, many other different numerical methods have been proposed to simulate such fractional operators [68]. Let us first consider the common notation for the Riesz-Feller derivative in terms of the Laplacian $\partial^z / \partial |x|^z := -(-\Delta)^{z/2}$ [69]. The matrix transform algorithm is based on the following definition. First consider

the usual finite-difference scheme for a Laplacian in one dimension

$$\Delta \phi(x) = \frac{1}{(\Delta x)^2} \{\phi(x - \Delta x) - 2\phi(x) + \phi(x + \Delta x)\}, \quad (15)$$

where $\{\phi(x)\}$ is the complete set of orthogonal functions. Using the Fourier transform $\phi(x) = \frac{1}{2\pi} \int \hat{\phi}(q) e^{-iqx} dq$, the discretized Laplacian (15) in the Fourier representation can be rewritten as

$$(\widehat{\Delta})\hat{\phi}(q) = -[2 - 2\cos(q\Delta x)]\hat{\phi}(q), \quad (16)$$

where Δx corresponds to the lattice constant.

One might start with the Fourier representation of the discretized Laplacian to approximate the Fourier representation of the discretized fractional Laplacian $(-\Delta)$ as $\lambda(q) = 2[1 - \cos(q)]$ and raise it to the appropriate power $\{2[1 - \cos(q)]\}^{z/2}$. This technique was invented by Ilic *et al.* (for more details see Refs. [66–68]).

The matrix transform approach proposes that one can obtain the elements of the matrix representation of the Laplacian $\mathbb{A}_{l,m} = -\int_0^{2\pi} \frac{dq}{2\pi} [2 - 2\cos(qa)] e^{iq(l-m)}$, where $\mathbb{A} \equiv \text{tridiag}(1, -2, 1)$. The elements of the matrix \mathbb{K} , representing the discretized fractional Laplacian $(-\Delta)^{z/2}$, are then

$$\begin{aligned} \mathbb{K}_{l,m} &= -\int_0^{2\pi} \frac{dq}{2\pi} e^{iq(l-m)} \{2[1 - \cos(q)]\}^{z/2} \\ &= \frac{\Gamma(-\frac{z}{2} + n)\Gamma(z + 1)}{\pi\Gamma(1 + \frac{z}{2} + n)} \sin\left(\frac{z}{2}\pi\right), \end{aligned} \quad (17)$$

where $n = |l - m|$ and fractional order $z \geq 1$. In the special case $z = 2$, the \mathbb{K} matrix is equal to the matrix \mathbb{A} of a simple Laplacian. On the other hand, if $\alpha/2$ is an integer, then $\mathbb{K}(n) = (-1)^{\alpha-n+1} C_{\alpha,\alpha/2+n}$ for $n \leq \alpha/2$ and $\mathbb{K}(n) = 0$ for $n > \alpha/2$, where $C_{\alpha,\alpha/2+n}$ are binomial coefficients [70].

Combining Eqs. (14) and (17) and substituting into Eq. (10) leads to the discrete version of the QGEM. We employ the finite-difference method to investigate the numerical discretization of Eq. (10), in the form

$$\begin{aligned} u_i^{n+1} &= u_i^n + \Delta t \left(\frac{1}{(\Delta x)^z} \sum_{j=0}^L \sum_{k=0}^L \Lambda(|i-j|) \mathbb{K}_{j,k} u_k^n \right. \\ &\quad \left. + F + f_p(x_i, u_i^n) \right), \end{aligned} \quad (18)$$

where u_i^n approximates the interface profile $u(x_i, t_n)$ at the i th lattice point and the n th time step. The lattice constant Δx has been set equal to one and the grid steps Δt in time have been chosen to be small enough to avoid numerical instabilities.

In order to numerically generate a quenched random field $f_p(x_i, u_i^n)$, without loss of generality we assume the continuous stochastic variables $u(x_i, t_n)$ are discretized into a finite numbers of integer values $[u_i^n/\epsilon]$, where $\epsilon \ll 1$ is an arbitrary small parameter and $[\dots]$ represents the bracket notation for the integer part of a given continuous variable. Then the quenched random field f_p is defined on a square array where each cell $[i, h]$ ($1 \leq i \leq L$ and $h = [u_i^n/\epsilon]$) is assigned an identically distributed random variable $\eta(i, h)$ with normal Gaussian distribution with zero mean and unit variance. The

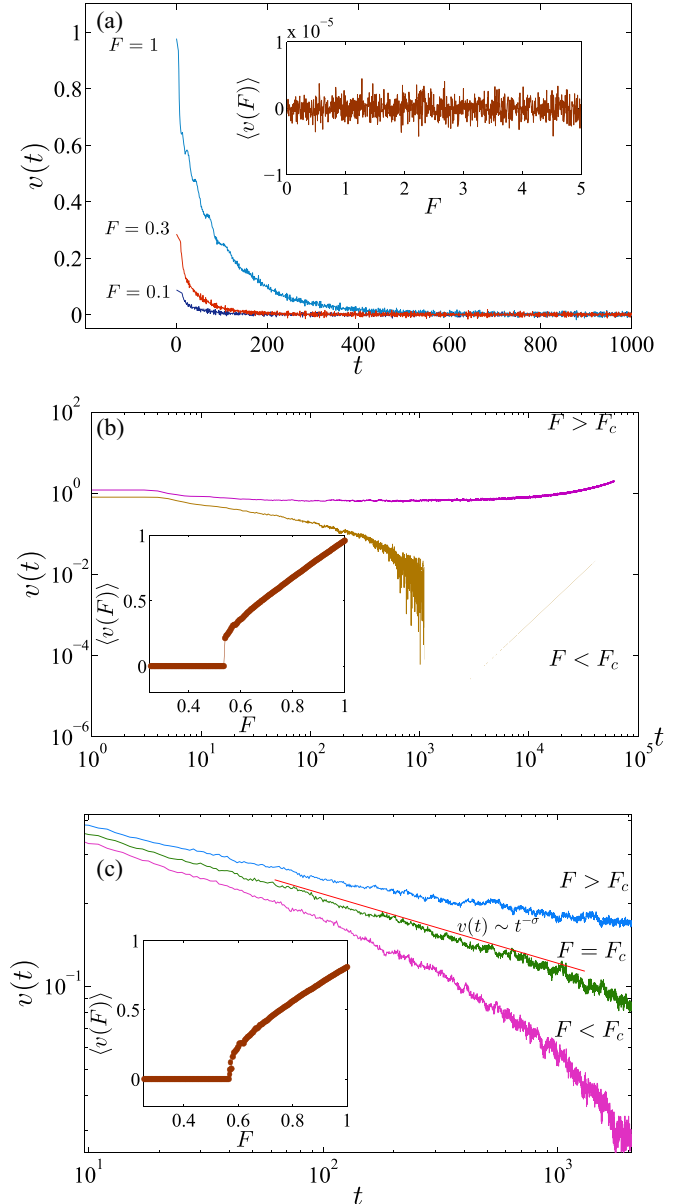


FIG. 1. Numerical evaluation for the average velocity $v(t, F) = \frac{d}{dt} \langle \int u(x, t) dx \rangle$ for the generalized elastic model with quenched disorder, which corresponds to the order parameter of the pinning-depinning transition of the viscoelastic interface driven through a disordered media. The behavior of the order parameter is strongly influenced by the hydrodynamic interaction parameter α and the fractional power z . (a) Order parameter $v(t)$ as a function of time for three different values of the external force F ; it goes to zero when $t \rightarrow \infty$. The saturation values of the order parameter $v(F)$ is shown in the inset. Note that there is no phase transition for the values $\alpha = 0.5$ and $z = 1.0$ in Eq. (10). (b) Order parameter as a function of time and force for the so-called first-order phase transition for the values $\alpha = 0.5$ and $z = 3.0$. (c) Same analysis as in (b) for the values $\alpha = 0.5$ and $z = 4.0$, showing an ordinary pinning-depinning phase transition. The red solid line corresponds to the scaling relation $v(t) \sim t^{-\sigma}$ for the critical point $F = F_c$.

random disorder $f_p(x_i, u_i^n)$ is obtained by the linear interpolation of the random force between two random variables $\eta(i, h)$ and $\eta(i, h + 1)$, where $h = [u_i^n/\epsilon]$.

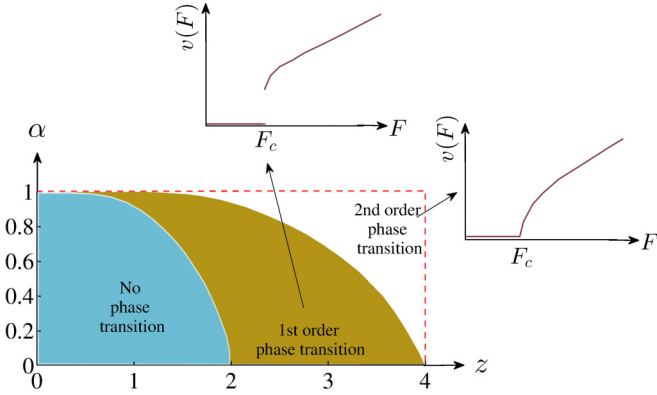


FIG. 2. Phase diagram of the generalized elastic model with quenched disorder. There are three different regimes, depending on the values of the parameters z and α in Eq. (10). The first regime is when $z \ll 4$ and $\alpha < 1$, where there is no phase transition between pinned and moving phases. The second regime is when $z < 4$ and $\alpha \gg 0$, where the order parameter of the system $v(F)$ as a function of the control parameter F changes continuously from zero to nonzero values (second-order phase transition). In the third regime the mean velocity $v(F)$ as a function of F changes discontinuously from zero to nonzero values (first-order phase transition).

The numerical investigation of the scaling characteristics and critical exponents of the quenched generalized elastic model for different values of the fractional order z and the nonlocal hydrodynamic interaction power α is presented in detail in the next section.

IV. NUMERICAL RESULTS

To determine the time evolution of the interface specified by $u(x, t)$ and to obtain the critical properties of the QGEM, the simulation is started with the initial

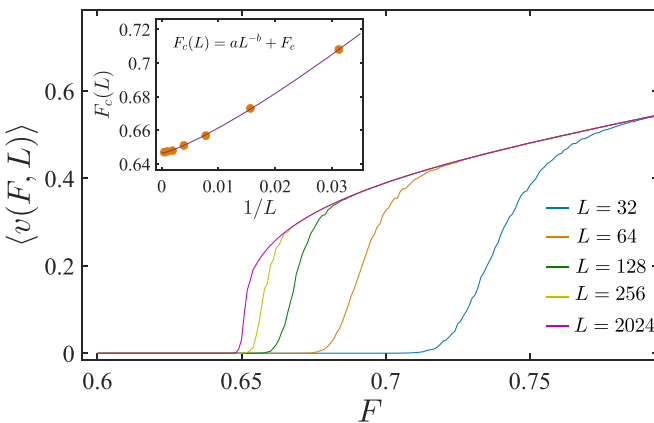


FIG. 3. Steady-state interface mean velocity v (for the QGEM with $z = 4$ and $\alpha = 1$) as a function of the driving force F and system size L . In order to determine the critical force F_c in the scaling limit $L \gg 1$, we measure the value $F_c(L)$, with $F = F_c(L)$ the transition point for a system with finite size L . The plot of $F_c(L)$ as a function of L is shown in the inset. The red solid line indicates $F_c(L) = aL^{-b} + F_c$, with $a = 4.513 \pm 0.005$, $b = 1.238 \pm 0.003$, and $F_c = 0.646 \pm 0.001$.

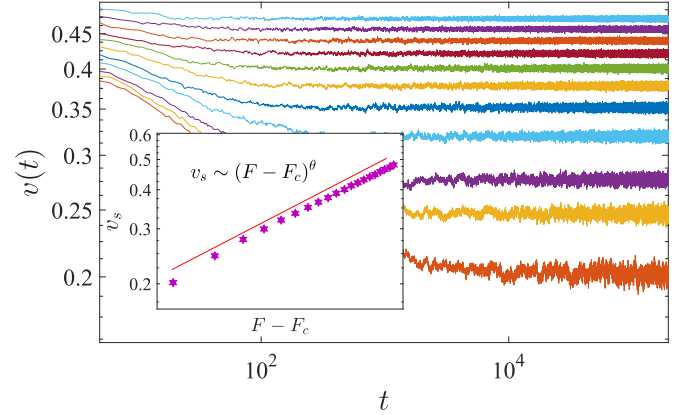


FIG. 4. A log-log plot of velocity $v(t)$ as a function of time t for various values of the external driving force $F > F_c$. In this region the mean velocity decreases in a power law at the beginning and then becomes constant at a later time. The log-log plot of the stationary state velocity v_s as a function of $F - F_c$ is shown in the inset. The red solid line represents $v_s \sim (F - F_c)^\theta$, with $\theta = 0.285 \pm 0.002$.

condition $u(x, 0) = 0$ and boundary condition $u(x, t) = u(x + L, t)$. We simulate this model on a lattice of size $L \in \{32, 64, 128, 256, 512, 1024, 2048\}$. In addition, we carefully choose the time increment Δt small enough to ensure the stability of the numerical algorithm.

In order to determine the criticality of the QGEM (10) and (18) for various parameter values of the fractional order z and the hydrodynamic interaction parameter α , we first compute the average velocity $v(t, F) = \frac{d}{dt} \langle \int u(x, t) dx \rangle$ as a function of time for various values of the external homogeneous force F .

Surprisingly, our simulations indicate that the QGEM in the limit $t \rightarrow \infty$ exhibits three quite different behaviors depending on the values of z and α . When hydrodynamic interactions are strongly long range $\alpha \ll 1$ and the

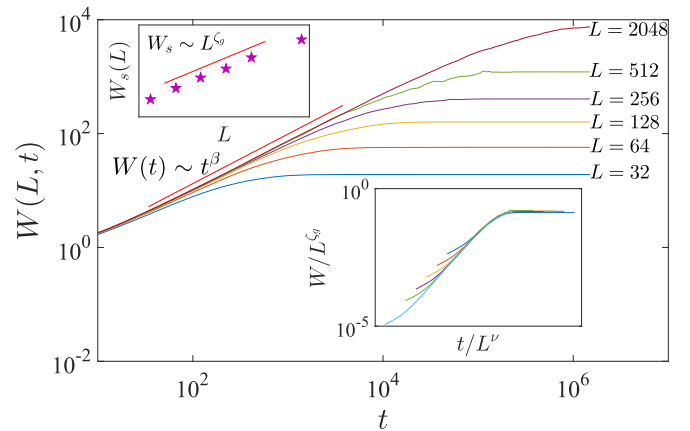


FIG. 5. A log-log plot of the interface width $W(L, t)$ vs t and different system size $L \in [32, 64, 128, 256, 512, 2048]$ for the QGEM with $z = 4$ and $\alpha = 1$. Results have been averaged over 10^4 noise realizations. The top inset shows a log-log plot of the saturated surface width W_s as a function of system size L and the bottom inset shows the best data collapse with the exponents $\xi_g = 1.358 \pm 0.004$ and $\nu = 1.625 \pm 0.005$.

TABLE I. Measured exponents from numerical simulation of the QGEM with local hydrodynamic interaction $\alpha = 1$ for different values of z at the critical depinning transition point $F = F_c$.

z	θ	β	ζ_g	ζ_l	σ
1.5	0.512 ± 0.005	0.877 ± 0.002	1.244 ± 0.003	0.915 ± 0.005	0.124 ± 0.003
2.0	0.445 ± 0.003	0.875 ± 0.003	1.255 ± 0.005	0.925 ± 0.004	0.125 ± 0.005
2.5	0.376 ± 0.004	0.869 ± 0.002	1.263 ± 0.004	0.935 ± 0.005	0.128 ± 0.002
3.0	0.315 ± 0.005	0.862 ± 0.002	1.268 ± 0.003	0.955 ± 0.003	0.134 ± 0.002
3.5	0.294 ± 0.004	0.851 ± 0.004	1.302 ± 0.004	0.990 ± 0.004	0.143 ± 0.003
4.0	0.285 ± 0.002	0.835 ± 0.003	1.358 ± 0.004	1.095 ± 0.005	0.155 ± 0.002

fractional power $z \ll 4$, there exists no phase transition between a pinned phase and a moving phase. In this regime $\lim_{t \rightarrow \infty} v(t, F) = 0$ for an arbitrary external driving force F . Such a behavior is shown in Fig. 1(a) for $\alpha = 0.5$ and $z = 1.0$.

In the opposite limit when the parameters $\alpha \leq 1$ and $z \gg 1$,

the velocity of the interface remains zero (pinned phase) up to a critical force F_c and above F_c the velocity $v(t)$ decreases as a power law at the beginning and then becomes constant at a later time, i.e., $\lim_{t \rightarrow \infty} \frac{d}{dt} v(t, F) = 0$ (moving phase). As indicated in Fig. 1(c), $v(F)$ is a continuous function of F . Thus the transition looks similar to the continuous phase transition in the context of the critical phenomena.

Another surprising feature of the QGEM is the anomalous pinning-depinning transition for some specific values of the parameters α and z in the (α, z) plane. In the anomalous regime, an elastic interface which exhibits nontrivial phase transition behavior is pinned when $F < F_c$. However, for $F > F_c$ we observe a jump in the average velocity as a function of F (see Fig. 1), which may lead to a first-order phase transition in which the order parameter of the system changes discontinuously from zero to a finite value. Note that above F_c the average velocity varies with time $\lim_{t \rightarrow \infty} \frac{d}{dt} v(t, F) \neq 0$, which is noticeably different from a standard pinning-depinning phase transition that appears in the elastic interface models. Figure 2 shows a phase diagram calculated for the generalized elastic model with quenched disorder.

We focus here on one aspect of the problem, namely, the scaling behavior with characteristic exponents of the QGEM close to the depinning critical point. Identifying the critical value F_c of the external driving force at the point when the infinite system becomes pinned is necessary since we are interested in the scaling behavior at the depinning transition. We measure the velocity of the average height $v(t, F)$ as a function of time for various values of the external driving

force F to calculate the critical force F_c . In the depinned zone $F > F_c$, $v(t)$ drops in a power law at first and then becomes constant later. In the pinned area of $F < F_c$, on the other hand, $v(t)$ decays quickly to zero. The average velocity of the stationary state depends on system size. In Fig. 3 we show the simulation results for several lattice sizes $32 \leq L \leq 2048$. In our model we estimate that the critical force $F_c(L)$ is well fitted by a power-law function $F_c(L) = aL^{-b} + F_c$, where F_c is the critical driving force in the scaling limit.

To determine the exponent θ , let us now analyze the time evolution of the interface velocity towards the final sliding steady state for $F > F_c$. In Fig. 4 we show the time evolution of $v(t)$ for forces above the threshold. We can distinguish two different regimes for the evolution of $v(t)$. In short time, $v(t)$ drops in a power law and then tends to a constant v_s . The inset of Fig. 4 shows the saturated velocity for various driving forces F in a logarithmic scale, which leads to $v_s \sim (F - F_c)^\theta$. We measure the exponent θ using this scaling relation; the values are reported in Tables I and II.

At the depinning threshold F_c , the depinned interface shows scaling behavior in the global interface width $W(L, t) \sim t^\beta f(L/t^{1/\nu})$, where L is the system size, β is the growth exponent, ν is the dynamical exponent, and $f(x)$ is a scaling function with $f(x) \sim x^{\zeta_g}$ for $x \ll 1$ and $f(x) \sim \text{const}$ for $x \gg 1$. We measure $W(L, t)$ as a function of time to calculate the dynamical roughness exponent β , regulating the rate of growth of the interface width, as illustrated in Fig. 5. The scaling exponent β is obtained by using the relation $W(t) \sim t^\beta$ for early time. On the other hand, the growth velocity of the average height at the critical point scales like $v(t) = d\bar{u}/dt \sim t^{-\sigma}$. Since $W \sim \bar{u}$, this results in a relation $v(t) \sim t^{\beta-1}$. Therefore, the exponents β and σ are not independent and the relation $\beta + \sigma = 1$ occurs. In Tables I and II we summarize our numerical findings for exponents β and σ for different values of control parameters z and α . Interestingly, the results

TABLE II. Measured exponents from numerical simulation of the QGEM with $z = 4$ and different values of nonlocal hydrodynamic interaction parameter α at the critical depinning transition point $F = F_c$.

α	θ	β	ζ_g	ζ_l	σ
1.0	0.285 ± 0.002	0.835 ± 0.003	1.358 ± 0.004	1.095 ± 0.005	0.155 ± 0.002
0.8	0.297 ± 0.004	0.704 ± 0.002	1.220 ± 0.003	1.010 ± 0.005	0.334 ± 0.001
0.6	0.311 ± 0.005	0.621 ± 0.004	1.107 ± 0.004	0.985 ± 0.004	0.427 ± 0.003
0.4	0.331 ± 0.006	0.556 ± 0.004	1.020 ± 0.004	0.980 ± 0.003	0.466 ± 0.003
0.2	0.361 ± 0.006	0.503 ± 0.005	0.954 ± 0.005	0.970 ± 0.005	0.486 ± 0.002

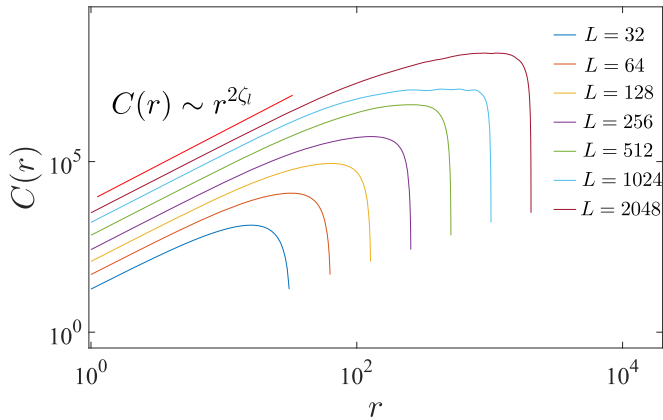


FIG. 6. Equal-time correlation function $C(r)$ for pinned QGEM interfaces slightly below threshold F_c . Here we consider the model with parameters $z = 4$ and $\alpha = 1$, but the results will be valid for the other values of z and α in the continuous phase transition regime. We average the data over 10^4 independent realizations. The scaling behavior $C(r) \sim r^{2\xi_l}$ is suppressed by the finite-size effect. The red solid line indicates the exponent $\xi_l = 1.095 \pm 0.005$.

are in good agreement with the prediction $\beta + \sigma = 1$. When the time exceeds the characteristic time $t_W^x \sim L^\nu$, the global interface width $W(L, t)$ reaches a saturation value $W_s(L)$. We use $32 \leq L \leq 2048$ to simulate various system sizes to obtain the roughness exponent ζ_g , which describes the saturation of the interface fluctuation. To determine the global roughness exponent ζ_g for QGEM we use the scaling relation $W_s(L) \sim L^{\zeta_g}$. We obtain ζ_g from the double-logarithmic plot of the saturated surface width as a function of the system size. The top inset in Fig. 5 depicts the saturated width W_s for different lattice sizes in a logarithmic scale. In Tables I and II we show the results for various values of z and α . In addition, the scaling plot of W/L^{ζ_g} versus t/L^ν for various system sizes demonstrates excellent data collapse, as shown in the bottom inset of Fig. 5.

Finally, to further investigate the scaling behavior of the QGEM and to evaluate the local roughness exponent ζ_l , we calculate the two-point correlation function $C(r)$ [see Eq. (3)]. The log-log diagram of $C(r)$ versus r as shown in Fig. 6 gives the slope ζ_l . Our computations are reported in Tables I and II. It seems that the local roughness exponent does not change with respect to the control parameters α and z and it is nearly constant and equal to unity.

V. CONCLUSION

In this paper we have studied the depinning transition of the elastic interface with nonlocal hydrodynamic interactions. As we mentioned earlier, this model is called generalized elastic model in the presence of quenched disorder. We numerically studied different aspects of this model for different values of the fractional order z and the nonlocal hydrodynamic interaction power α . We found that the behavior of the order parameter $v(F)$ as a function of the external force F highly depends on the values of z and α . There are three distinct phases in the z - α phase space. For small values of z and α the order parameter vanishes and in the thermodynamic limit the steady-state order parameter approaches zero. In the opposite limit, where $\alpha \sim 1$ and $z \gg 1$, the model exhibits a second-order phase transition and the order parameter $v(F)$ continuously changes from zero to nonzero values. Finally, there is an additional phase when the order parameter changes discontinuously from zero to nonzero values, which is characterized by a first-order phase transition. We have analyzed in detail the steady state of the model in the second-order phase transition regime. Our model displays naturally scaling features near the critical point F_c . We measured different scaling exponents as functions of z and α . Our results are in good agreement with the well-known models.

Many open questions remain. First, it will be interesting to apply this numerical algorithm to other relevant aspects of interface dynamics with nonlocal hydrodynamic interactions in the presence of quench disorder, such as developing numerical tools to study this model in a d -dimensional space. Second, we would like to study the system in detail when it exhibits a first-order phase transition in which the order parameter of the system changes discontinuously from zero to a finite value (see Fig. 2). It would be interesting to investigate the hysteretic response of the QGEM [71,72]. Another interesting direction would be to extend numerical tools to study the QGEM with nonlinear terms [38,39].

ACKNOWLEDGMENTS

We would like to thank A. Chechkin for early discussions and the two anonymous referees for their insightful comments and suggestions that helped improve our manuscript.

- [1] M. Kardar, *Phys. Rep.* **301**, 85 (1998).
- [2] D. S. Fisher, *Phys. Rep.* **301**, 113 (1998).
- [3] L. A. N. Amaral, A.-L. Barabási, H. A. Makse, and H. E. Stanley, *Phys. Rev. E* **52**, 4087 (1995).
- [4] H. Kawamura, T. Hatano, N. Kato, S. Biswas, and B. K. Chakrabarti, *Rev. Mod. Phys.* **84**, 839 (2012).
- [5] D. Marković and C. Gros, *Phys. Rep.* **536**, 41 (2014).
- [6] G. Ódor, *Rev. Mod. Phys.* **76**, 663 (2004).
- [7] C. Le Priol, J. Chopin, P. Le Doussal, L. Ponsou, and A. Rosso, *Phys. Rev. Lett.* **124**, 065501 (2020).
- [8] H. Gao and J. R. Rice, *J. Appl. Mech.* **56**, 828 (1989).
- [9] J. Schmittbuhl, S. Roux, J. P. Vilotte, and K. J. Maloy, *Phys. Rev. Lett.* **74**, 1787 (1995).
- [10] A. Tanguy, M. Gounelle, and S. Roux, *Phys. Rev. E* **58**, 1577 (1998).
- [11] M. J. Alava, P. K. Nukala, and S. Zapperi, *Adv. Phys.* **55**, 349 (2006).
- [12] D. S. Fisher, *Phys. Rev. B* **31**, 1396 (1985).
- [13] G. Grüner, *Rev. Mod. Phys.* **60**, 1129 (1988).
- [14] G. Blatter, M. V. Feigel'man, V. B. Geshkenbein, A. I. Larkin, and V. M. Vinokur, *Rev. Mod. Phys.* **66**, 1125 (1994).

- [15] S. Lemerle, J. Ferré, C. Chappert, V. Mathet, T. Giamarchi, and P. Le Doussal, *Phys. Rev. Lett.* **80**, 849 (1998).
- [16] T. Tybell, P. Paruch, T. Giamarchi, and J. M. Triscone, *Phys. Rev. Lett.* **89**, 097601 (2002).
- [17] M. Cieplak and M. O. Robbins, *Phys. Rev. Lett.* **60**, 2042 (1988).
- [18] S. Moulinet, A. Rosso, W. Krauth, and E. Rolley, *Phys. Rev. E* **69**, 035103(R) (2004).
- [19] M. Alava, M. Dubé, and M. Rost, *Adv. Phys.* **53**, 83 (2004).
- [20] H. S. Rabbani, V. Joekar-Niasar, T. Pak, and N. Shokri, *Sci. Rep.* **7**, 4584 (2017).
- [21] B. K. Primkulov, A. A. Pahlavan, X. Fu, B. Zhao, C. W. MacMinn, and R. Juanes, *J. Fluid Mech.* **875**, R4 (2019).
- [22] J. P. Sethna, K. A. Dahmen, and C. R. Myers, *Nature (London)* **410**, 242 (2001).
- [23] D. Bonamy, S. Santucci, and L. Ponson, *Phys. Rev. Lett.* **101**, 045501 (2008).
- [24] D. Cule and T. Hwa, *Phys. Rev. Lett.* **77**, 278 (1996).
- [25] A. Vanossi, N. Manini, M. Urbakh, S. Zapperi, and E. Tosatti, *Rev. Mod. Phys.* **85**, 529 (2013).
- [26] D. S. Fisher, K. Dahmen, S. Ramanathan, and Y. Ben-Zion, *Phys. Rev. Lett.* **78**, 4885 (1997).
- [27] A. Brú, S. Albertos, J. A. López García-Asenjo, and I. Brú, *Phys. Rev. Lett.* **92**, 238101 (2004).
- [28] B. Moglia, E. V. Albano, and N. Guisoni, *Phys. Rev. E* **94**, 052139 (2016).
- [29] A. L. Barabási and H. E. Stanley, *Fractal Concepts in Surface Growth* (Cambridge University Press, Cambridge, 1995).
- [30] *Scale Invariance, Interfaces, and Non-Equilibrium Dynamics*, edited by A. McKane, M. Droz, J. Vannimenus, and D. Wolf, NATO Advanced Studies Institute, Series B: Physics (Springer, New York, 2013), Vol. 344.
- [31] J. Krug, *Adv. Phys.* **46**, 139 (1997).
- [32] J. J. Ramasco, J. M. López, and M. A. Rodríguez, *Phys. Rev. Lett.* **84**, 2199 (2000).
- [33] I. G. Szendro, J. M. López, and M. A. Rodríguez, *Phys. Rev. E* **76**, 011603 (2007).
- [34] A. Rosso and W. Krauth, *Phys. Rev. E* **65**, 025101 (2002).
- [35] L. Laurson, S. Santucci, and S. Zapperi, *Phys. Rev. E* **81**, 046116 (2010).
- [36] P. Moretti, M. C. Miguel, M. Zaiser, and S. Zapperi, *Phys. Rev. B* **69**, 214103 (2004).
- [37] S. G. Samko, A. A. Kilbas, and O. I. Marichev, *Fractional Integrals and Derivatives, Theory and Applications* (Gordon and Breach, Amsterdam, 1993); I. Podlubny, *Fractional Differential Equations* (Academic, London, 1999); A. A. Kilbas, H. M. Srivastava, and J. J. Trujillo, *Theory and Applications of Fractional Differential Equations* (Elsevier, Amsterdam, 2006).
- [38] A. Alés and J. M. López, *Phys. Rev. E* **104**, 044108 (2021).
- [39] V. H. Purrello, J. L. Iguain, and A. B. Kolton, *Phys. Rev. E* **99**, 032105 (2019).
- [40] H. Leschhorn, *Physica A* **195**, 324 (1993).
- [41] A. Rosso and W. Krauth, *Phys. Rev. Lett.* **87**, 187002 (2001).
- [42] F. Lacombe, S. Zapperi, and H. J. Herrmann, *Phys. Rev. B* **63**, 104104 (2001).
- [43] A. Rosso, A. K. Hartmann, and W. Krauth, *Phys. Rev. E* **67**, 021602 (2003).
- [44] A. B. Kolton, A. Rosso, E. V. Albano, and T. Giamarchi, *Phys. Rev. B* **74**, 140201(R) (2006).
- [45] A. B. Kolton, G. Schehr, and P. Le Doussal, *Phys. Rev. Lett.* **103**, 160602 (2009).
- [46] E. E. Ferrero, S. Bustingorry, A. B. Kolton, and A. Rosso, *C. R. Phys.* **14**, 641 (2013).
- [47] E. E. Ferrero, S. Bustingorry, and A. B. Kolton, *Phys. Rev. E* **87**, 032122 (2013).
- [48] J. H. Lee, S. K. Kim, and J. M. Kim, *Phys. Rev. E* **62**, 3299 (2000).
- [49] C. Lee and J. M. Kim, *Phys. Rev. E* **73**, 016140 (2006).
- [50] H. H. Boltz and J. Kierfeld, *Phys. Rev. E* **90**, 012101 (2014).
- [51] H. Xia, G. Tang, D. Hao, and Z. Xun, *Eur. Phys. J. B* **85**, 315 (2012).
- [52] H. Haidara, B. Lebeau, C. Grzelakowski, L. Vonna, F. Biguenet, and L. Vidal, *Langmuir* **24**, 4209 (2008).
- [53] M. V. D'Angelo, G. Picard, and M. E. Poitzsch, J. P. Hulin, and H. Auradou, *Transp. Porous Media* **84**, 389 (2010).
- [54] J. Nissen, K. Jacobs, and J. O. Rädler, *Phys. Rev. Lett.* **86**, 1904 (2001).
- [55] P. Verma, M. D. Mager, and N. A. Melosh, *Phys. Rev. E* **89**, 012404 (2014).
- [56] D. S. Clague and R. J. Phillips, *Phys. Fluids* **8**, 1720 (1996).
- [57] M.-C. Miguel, J. S. Andrade, and S. Zapperi, *Braz. J. Phys.* **33**, 557 (2003).
- [58] B. Cui, H. Diamant, B. Lin, and S. A. Rice, *Phys. Rev. Lett.* **92**, 258301 (2004).
- [59] M. Sbragaglia, L. Biferale, G. Amati, S. Varagnolo, D. Ferraro, G. Mistura, and M. Pierno, *Phys. Rev. E* **89**, 012406 (2014).
- [60] A. Stannard, *J. Phys.: Condens. Matter* **23**, 083001 (2011).
- [61] A. Taloni, A. Chechkin, and J. Klafter, *Phys. Rev. Lett.* **104**, 160602 (2010).
- [62] A. Taloni, A. Chechkin, and J. Klafter, *Phys. Rev. E* **82**, 061104 (2010).
- [63] A. Taloni, A. Chechkin, and J. Klafter, *Europhys. Lett.* **97**, 30001 (2012).
- [64] A. Taloni, A. Chechkin, and J. Klafter, *Phys. Rev. E* **84**, 021101 (2011).
- [65] A. Taloni, A. Chechkin, and J. Klafter, *Math. Model. Nat. Phenom.* **8**, 127 (2013).
- [66] M. Ilic, F. Liu, I. Turner, and V. Anh, *Fract. Calc. Appl. Anal.* **8**, 323 (2005).
- [67] M. Ilic, F. Liu, I. Turner, and V. Anh, *Fract. Calc. Appl. Anal.* **9**, 333 (2006).
- [68] Q. Yang, Novel analytical and numerical methods for solving fractional dynamical systems, Ph.D. thesis, Queensland University of Technology, 2010.
- [69] A. I. Saichev and G. M. Zaslavsky, *Chaos* **7**, 753 (1997).
- [70] A. Zoia, A. Rosso, and M. Kardar, *Phys. Rev. E* **76**, 021116 (2007).
- [71] M. C. Marchetti and K. A. Dahmen, *Phys. Rev. B* **66**, 214201 (2002).
- [72] V. H. Purrello, J. L. Iguain, V. Lecomte, and A. B. Kolton, *Phys. Rev. E* **102**, 022131 (2020).